Morphological, mechanical and antibacterial properties of Ti–Cu–N thin films deposited by sputtering DC

Ihwanul Aziz [a,b], Emy Mulyani [b], Yusril Yusuf [a,*]

[a] *Department of Physics, Faculty of Mathematics and Natural Science, Universitas Gadjah Mada, Yogyakarta, Indonesia*
[b] *Research Center for Accelerator Technology, Research Organization of Nuclear Energy, National Research and Innovation Agency (BRIN), Yogyakarta, 55281, Indonesia*

A B S T R A C T

The problems associated with Stainless Steel 316 L (SS 316 L) orthopedic implants, when implanted in the human body, are infection, local inflammation, and the possibility of bacterial growth. In this study, SS 316 L was coated with copper-doped Titanium Nitride (Ti–Cu–N) using the DC Sputtering technique. This Ti–Cu–N film improved the antibacterial performance and mechanical properties of SS 316 L. The Ti–Cu–N films were deposited using reactive DC sputtering with an 80%:20% argon to nitrogen ratio. The source voltage and current were kept constant at 10 kV and 10 mA, respectively. X-Ray Diffraction (XRD) showed that the phases formed were TiN and Cu with FCC crystal structure. Results show that the surfaces of samples containing 44.34 wt% and 54.97 wt% Cu had antibacterial effectiveness against *Staphylococcus aureus* (S. Aureus). The highest hardness value of a Ti–Cu–N layer was 212.032 Vickers Hardness Number (VHN), which was an improvement of 36.63% on the raw material (155.18 VHN). Surface morphology analysis using SEM-EDS was performed on the samples before and after the antibacterial test to investigate the antibacterial mechanism of the surfaces of SS 316 L containing Ti–Cu–N against S. Aureus.

1. Introduction

Biomaterials are synthetic or natural materials in the form of ceramic polymers, or a combination of these materials, which can restore or replace body parts to improve human health. Depending on the application, biomaterials may need to be biocompatible, biodegradable, or bioabsorbable [1]. The most widely used metal-based biomaterials are stainless steel 316 L (SS 316 L), titanium alloy, and alloy Co-Cr [2]. Stainless steel is one of the materials widely used in the health care environment. However, it lacks antibacterial properties which limits its practical applications [3]. The deposition of antibacterial films on the material's surface is an effective way of improving the biomaterial quality of stainless steel [4]. One excellent material for modifying the surface of medical implants, such as dental implants, joint prostheses, and artificial joints, is Titanium Nitride (TiN) [5] as it possesses excellent corrosion resistance and favorable tribological properties [6,7]. A third element, such as silver or copper, can be added to the TiN to allow for the formation of the desired structure and nature [8]. It has been reported that silver ion has a bactericidal effect on more than 16 species of bacteria, while copper (Cu) ion is effective against other bacteria [9,10].

Copper ions can also increase the activity of osteoblasts and promote the proliferation and deposition of osteoblast collagen [11].

---

* Corresponding author.
  E-mail address: yusril@ugm.ac.id (Y. Yusuf).

Thus, the biological functions and unique properties of copper have attracted the attention of many researchers in the field of bone implants [12,13]. Furthermore, copper is an essential element in the human body and is very beneficial in physiological systems [14]. Its low toxicity properties on the right weight percent and good biological function make it the choice of doping agent for the improvement of antibacterial properties of biomaterials [15].

Many researchers have studied Ti–Cu–N films for biomaterial applications as these films enhance the antibacterial, mechanical and tribological properties of TiN films [16]. Various techniques can be used to deposit Ti–Cu–N, including DC Magnetron Sputtering [6,7, 16,17], plasma surface alloying [18], pulse biased arc ion plating [19], arc ion plating [20], and arc ion deposition [21], all of which result in an increase in the antibacterial properties of biomaterials. However, all of these techniques require complicated preparation and technology for the Cu doping process on TiN films. This inspired the researchers of this study to investigate making Ti–Cu–N films for better antibacterial and mechanical properties via a simple and practical method - using reactive sputtering. Insertion was carried out using a thin plate of Cu as an antibacterial element. The thin plate of Cu was placed directly on the surface of the sputtering target, and then the sputtering process was carried out. This deposition technique has never been carried out before, especially with Ti–Cu–N, for the purpose of increasing the antibacterial properties of SS 316 L implant biomaterial. This technique can also be applied to other antibacterial elements, such as silver (Ag). In this study reported the results of morphological analysis, antibacterial and mechanical properties of SS 316 L coated with Ti–Cu–N.

2. Experimental

2.1. Materials and methods

TiN films with various Cu atomic contents were prepared using a reactive sputtering system. SS316L foils with a mirror polish on one side (Goodfellow FF210376) and a size of 10×10 mm with a thickness of 0.9 mm were used as the substrate. These had a Vickers Hardness Number (VHN) of 155.18. Table 1 shows the chemical composition of SS 316 L from EDS data. A high purity titanium 99.99% (Goodfellow TI009300) disk with a diameter of 50 mm and a thickness of 3 mm was used as the sputtering target. High purity Cu foil 99.99% (Goodfellow CU000570) was processed to sizes of 5, 7.5, 10, 12.5, and 15 mm with a thickness of 0.1 mm for the doping. The Cu was shaped in a circle to avoid electrical discharge from high voltage. Table 2 shows a sample code with the deposition parameters of the Ti–Cu–N films. The standby vacuum was 2.5×10^{-4} mbar, and the constant working pressure of the sputtering was 2×10^{-2} mbar. The substrate was cleaned with an ultrasonic cleaner for 10 min using soap, water, and ethanol. The Ti–Cu–N films were deposited by reactive DC sputtering with an 80%:20% ratio of argon to nitrogen gas. The source voltage and current were kept constant at 10 kV and 10 mA, respectively. The optimization of the sputtering parameters of TiN based on hardness is shown in Fig. 1 and the greatest hardness was achieved in 2 h. This is in line with research on corrosion resistance which has also shown achievement of the greatest hardness in 2 h [22]. The Cu content of the Ti–Cu–N films was controlled by varying the diameter of Cu foil put directly on the surface sputtering target.

2.2. Structure and surface characteristics of Ti–Cu–N films

The surface morphology of the Ti–Cu–N films on SS 316 L was observed using a Scanning Electron Microscope (SEM) Hitachi SU-3500. The chemical composition of the Ti–Cu–N films with different Cu contents on the SS 316 L surface was analyzed using Energy-Dispersive X-ray spectroscopy (EDS). Film thickness was investigated using Field Emission Scanning Electron Microscopes (FE-SEM) JEOL JIB-4610F. The crystal structure of the Ti–Cu–N was determined using X-ray diffraction (XRD PANalytical) with 1.5410 Cu Kα.

2.3. Mechanical and adhesion characterization

Hardness was measured using a digital hardness Vickers tester (Matsuzawa MMT-X7) with an indentation time of 10 s and an indenter load of 1 g. The test was carried out at 10 points, and then the results were averaged. The thin film adhesion test was carried out qualitatively using the Rockwell C Adhesion test based on standard VDI Guidelines 3198 [23]. After indenting using Rockwell C, observation and analysis of damage to the thin layer was conducted via visual observations through an optical microscope. The results of visual observations are compared in Fig. 2. HF 1 – HF 4 show results of good adhesion strength, while HF 5 – HF 6 show poor adhesion strength.

2.4. Antibacterial test

The test method used was based on JIS Z 2801: 2000 Antimicrobial products – Test for antimicrobial activity and efficacy with modification. A *Staphylococcus aureus* bacteria suspension was prepared by inoculation of 1 loop of *Staphylococcus aureus* bacteria in

Table 1
Chemical Composition Stainless Steel 316 L from EDS data.

Raw Material	Fe (wt.%)	Cr (wt.%)	Ni (wt.%)	Mo (wt.%)	Others (wt.%)
SS 316 L	70.45	17.05	10.44	1.94	0.12

Table 2
Deposition parameter of Ti–Cu–N films.

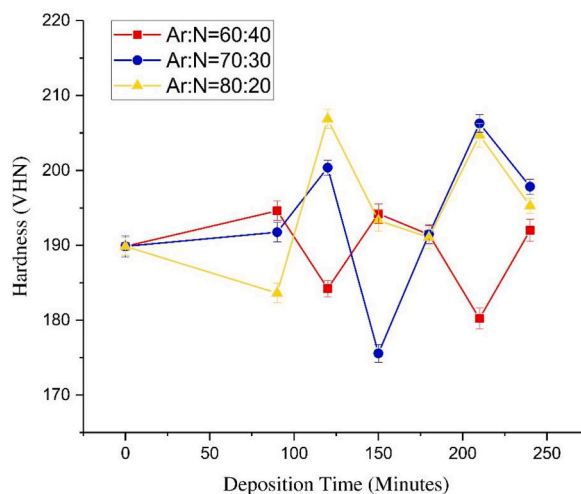| Sample Code	Cu plate diameter (mm)	Deposition Time (Minutes)
S1	5	120
S2	7.5	120
S3	10	120
S4	12.5	120
S5	15	120

Fig. 1. Vickers hardness for optimation deposition time and gas comparation (Ar:N$_2$) sputtering parameter TiN films.
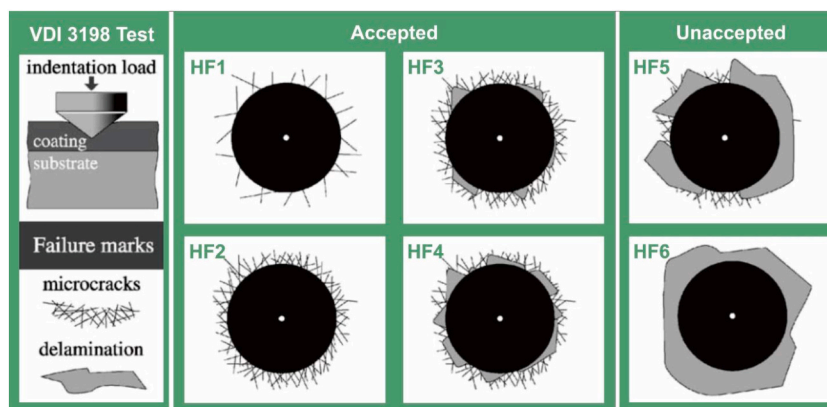
Fig. 2. Classification into the adhesion classes HF 1 to HF 6 by using the Rockwell-indentation method according to VDI 3198 [23].

nutrient broth, which was incubated at room temperature and in a shaker of concentration 5×10^8 colony-forming units per milliliter (cfu/mL). The metal plate sample was placed in a sterile Petri dish, then sterilized using ultraviolet for 15 min. A total of 50 µL of *Staphylococcus aureus* bacterial suspension was inoculated on the surface of the film and of the control samples. Petri dishes containing the pieces of test metal and inoculated bacteria were incubated at 37 °C with a humidity of ±90% for 24 h. After incubation, the metal plates containing the *Staphylococcus aureus* bacteria were washed using 10 mL of phosphate-buffered saline solution. To count the number of bacterial cells, a 10-fold serial dilution of the sample was carried out until the dilution reached 1×10^5 and the agar plate culture method were used. Using the jelly plate culture method, 0.1 mL of the diluted solution was inoculated on a nutrient jelly medium on a spread plate using an aseptic Drigalsky. This was then incubated at a temperature of 37 °C for 24 h. After incubation, the number of visible bacterial colonies was counted using a colony counter. To determine antimicrobial performance, the following equation was used [18]:

$$\text{Reduction}\ (\%):[(\lambda_0-\lambda_t)\ /\ \lambda_0]\times100\%$$

where λ_t (expressed in cfu) represents the number of bacterial cells in the sample and λ_0 represents the number of the uncoated reference sample (SS316L). The test was repeated three times then the average value is taken.

3. Result and discussion

3.1. Structure and element distributions

Fig. 3 shows the XRD pattern of the Ti–Cu–N film on the surface of SS 316 L. The diffraction peaks of FCC TiN crystals appeared at 2θ angles around 36.6° TiN (111), 61.89° TiN (220), and 74.1° TiN (311), according to the ICDD cards 00-031-1403. The diffraction peaks of FCC Cu crystals were seen at 2θ around 50.37° Cu (200) and 73.9° Cu (220), according to the ICDD card 00-002-1225. This XRD pattern is similar to the results of other research [[18]; however, at an angle of 74.1°, TiN (311) coincides with Cu (220). Based on the XRD data, the Ti–Cu–N film wholly adhered to the surface of SS 316 L, giving only two types of crystalline phases in the Ti–Cu–N film, namely the TiN and Cu phases. In samples S3, S4, and S5, the TiN (111) peak appeared at 36.6° and was the highest peak in sample S5. This peak did not appear at all in samples S1 and S2. Based on the results of the EDS of samples S1 to S5, the Cu composition increased in proportion to the size of the disk diameter. In S5, the Cu composition decreased slightly, but the intensity of the XRD peak at TiN (111) increased. This indicates that Cu composition does not affect crystal growth but triggers the emergence of TiN (111) at an angle of 36.6°. The appearance of the TiN (111) peak does not affect the intensity of other peaks. Cu affects the formation of the TiN phase: the greater the Cu concentration, the greater the intensity of the TiN phase. In samples S1 and S2, the amount of Cu deposited was still small, so the TiN phase formed was also still small, and only certain crystal planes reflected X-rays. When more TiN phases were formed, the probability that plane (111) reflected X-ray diffraction was higher, and so S3– S5 formed the TiN phase (111) [24]. CuN bonding did not appear. Instead, it was Ti that made a stronger bond, meaning that formation of TiN was easier than CuN [19,24, 25].

Fig. 4 shows the content of the Ti–Cu–N elements in the film. Fig. 4 (a) displays data of the Ti–Cu–N elements in the sample before the antibacterial test. Based on this data, Cu content from S1–S4 increased from 7.4 wt% to 54.97 wt%, then dropped to 44.34 wt% in S5. Ti content from S1–S4 decreased from 12.82 wt% to 4.51 wt%, then increased to 9.85 wt% in S5. The nitrogen content in S1–S3 was stable at 5 wt%, but it fell in S4–S5 to 4.3 wt% and 4.5 wt%, respectively. Thus, as the diameter of Cu increases, the content of Ti–Cu–N elements appears to rise and fall. Ti and N displayed similar trends in that they decreased in amount in S1–S4 and then rose in S5. The number of Cu element that deposited to the sample is greater than Ti because the sputtering yield of Cu is greater than Ti [26]. In S5, the amount of Cu decreased due to the process of Cu deposition; when the formation of Ti–Cu–N reaches saturation, no more can be deposited. This is related to the properties of Cu bonds which aren't as strong in the Ti–Cu–N layer [25].

Fig. 4 (b) displays data of the Ti–Cu–N elements in the sample after the antibacterial test. It can be seen that the amount of Cu from S1–S3 increased from 6.13 wt% to 14.4 wt%, then dropped in S4–S5 to 8.5 wt% and 6.8 wt%, respectively. The amount of Ti fluctuated between S1–S5, with the lowest content being in S3, which was 2.5 wt%. Cu content decreased significantly in S4–S5, which is the result of the release of Cu ions to kill bacteria [27,28]. Nitrogen content increased after the antibacterial test as evidenced by the elemental data before the antibacterial test on S3–S4. The addition of nitrogen elements to S3 and S4 was caused by *S. Aureus* bacterial carcass contamination because the bodies of *S. Aureus* bacteria are composed of peptidoglycan guanine and cytosine, which contain nitrogen [29].

Fig. 5(S1–S5) illustrates the surface morphology of SEM analysis of the Ti–Cu–N films before the antibacterial test was carried out.
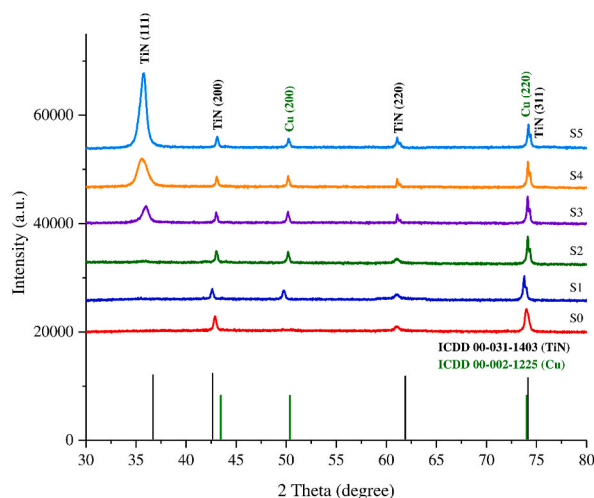

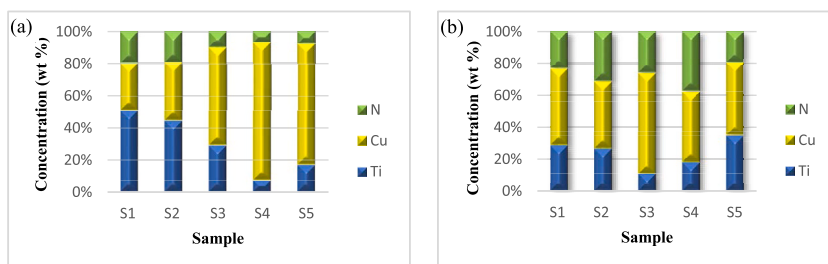**Fig. 3.** XRD patterns obtained for each Ti–Cu–N film.

Fig. 4. Ti–Cu–N composition of the sample analyzed by EDS: (a) Before antibacterial activity testing, (b) After antibacterial activity testing.

Raw refers to the surface morphology of the sample surfaces without Ti–Cu–N film. In this analysis, the particle size in S1–S4 can be seen to gradually decrease because the Cu content increases. Even in S4, tiny particles were observed attaching themselves together to form clusters like islands. In S5, particle size increased again because the amount of Cu decreased as compared to the EDS data of S5. As shown in Fig. 5 (S2, S3, S5), a rather large grain was observed which was unlike the original grain arrangement. Differences in grain size are caused by structural deviations on the surface of the substrate and the stocking fault of the neighbor during the deposition process [30].

Fig. 6(S1–S5) shows the morphology of the cross-sectional SEM images of samples. The average film thickness for S1–S5 was 0.618, 1.238, 0.558, 0.674, and 0.626 μm, respectively. The morphology of the cross-section displayed a distinctive dense structure with a well-defined film interface, this is similar to the results of other research [31]. The gap width between the film and substrate of samples S1–S5 gradually turned narrow. The addition of Cu can affect the growth mode of TiN and inhibit the gap film interface from width becoming narrow. There was an irregular layer of Ti–Cu–N; the irregularity of this layer was caused by specific defects on the surface of the substrate [30].

Fig. 7(S1–S5) shows the surface morphology of samples after the antibacterial test. Compared to the morphology before the antibacterial test, the surfaces of S1–S5 changed significantly. The granules on the surface of the layer were not visible because they had formed different patterns. This morphological change was caused by bacterial carcasses on the sample's surface. Surface patterns observed in S3–S4 resembled the morphological form of *S. Aureus* bacteria [32]. In S5, the bacterial carcass was visible but did not have the bacterial pattern shape of S3–S4. This indicates that increasing Cu concentrations kill bacteria at greater speeds.

Fig. 8(S1–S5) shows the distribution of elements N, Ti, and Cu on the sample surface. Although not dominant, the blue and pink Ti and N elements appeared relatively evenly distributed on the surfaces of samples S1–S5. Based on the EDS mapping data of Cu concentrations on the surface of sample S1, a green color could be seen accumulating in the middle of the sample surface. This shows that the Cu tended to accumulate in the middle of the sample. Sample S4 had the greatest Cu content, evidenced by the stronger green color it had than the other samples. For samples S2, S3, and S5, Cu concentrations were fairly evenly spread on the sample surface.
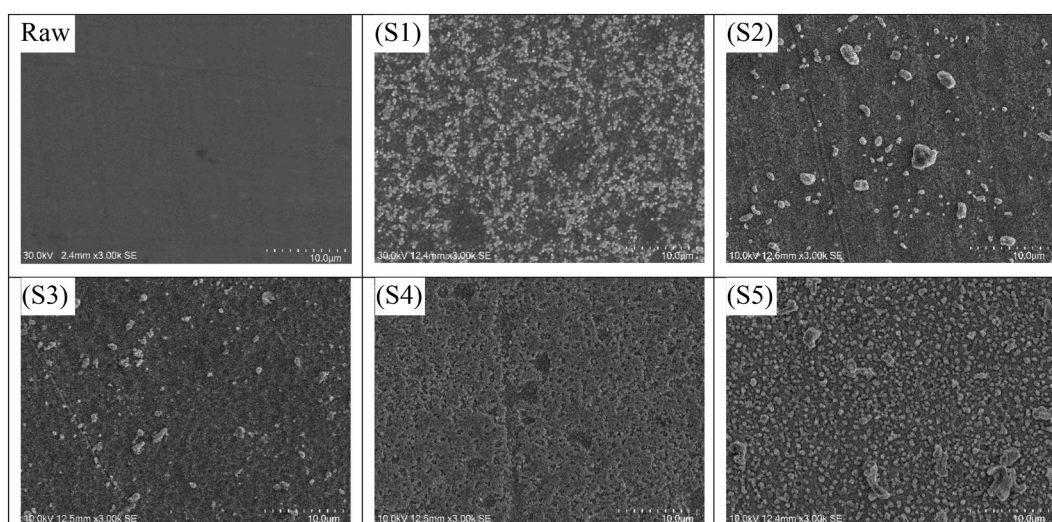

Fig. 5. SEM images of the films with varying Cu plate diameter before antibacterial activity testing: (Raw) SS316L uncoated, (S1) 5 mm, (S2) 7.5 mm, (S3) 10 mm, (S4)12.5 mm, (S5) 15 mm.
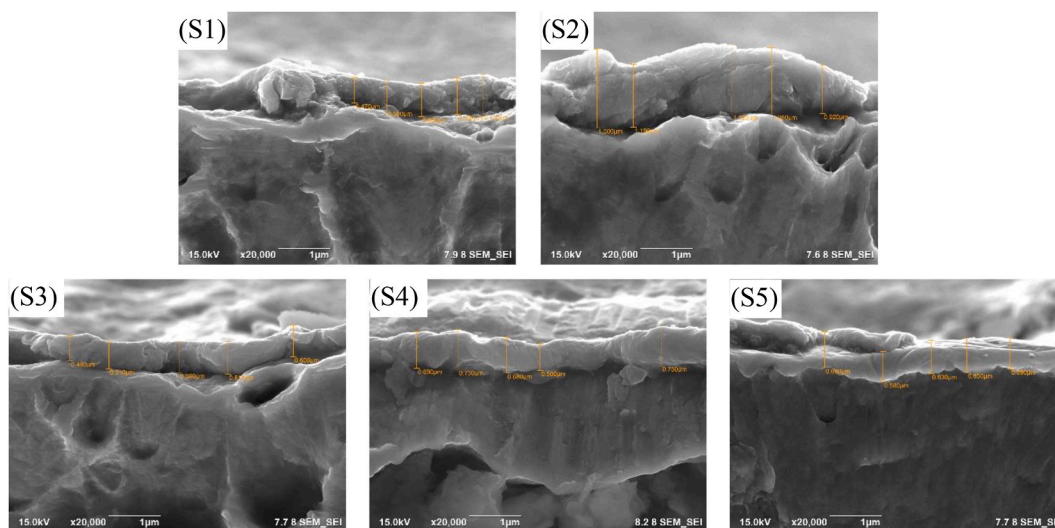
Fig. 6. Cross-sectional SEM images of the samples with varying Cu plate diameter before antibacterial activity testing: (S1) 5 mm, (S2) 7.5 mm, (S3) 10 mm, (S4)12.5 mm, (S5) 15 mm.
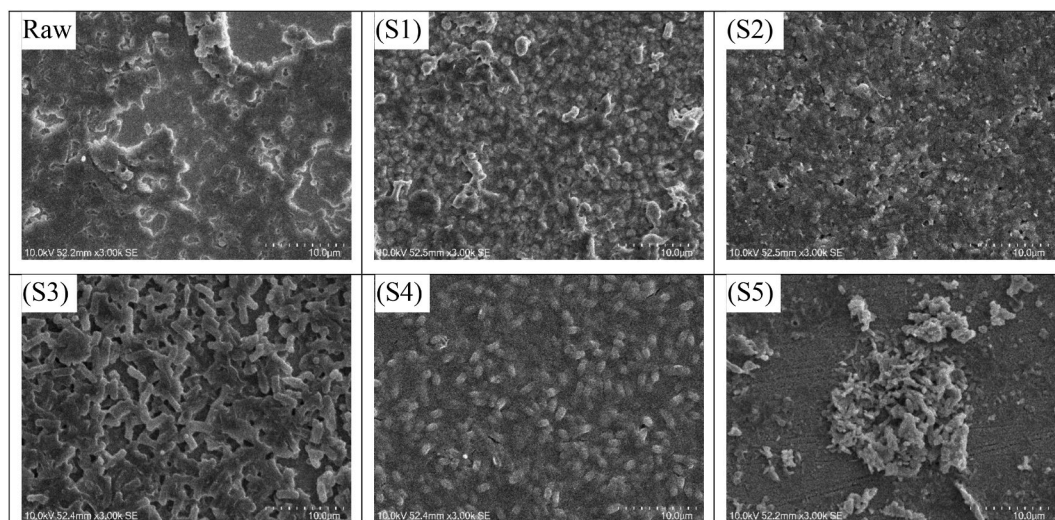

Fig. 7. SEM images of the films with varying Cu plate diameter after antibacterial activity testing: (Raw) SS316L uncoated, (S1) 5 mm, (S2) 7.5 mm, (S3) 10 mm, (S4)12.5 mm, (S5) 15 mm.

3.2. Mechanical and adhesion measurement

Fig. 9 displays Vickers hardness data for samples S1– S5. The test data in Fig. 9 is an average of 10 measurements. In S1–S4, hardness decreased from 212.032 VHN to 187.97 VHN; however, it increased in S5 to 197.77. When Cu content is low, Ti–N bonds increase near Cu atoms, thereby increasing hardness. Conversely, according to the Theory of Weak Bonds, the hardness of Ti–Cu–N decreases when Cu content increases [24]. The grain size and crystal structure affect hardness value of thin films [33]. Adhesion is the ability of two dissimilar particles to attract. The adhesion ability of thin films can be measured in several ways. One of these ways is qualitative measurement using the Rockwell C Adhesion Test approach. This test damages the thin layer causing cohesive and adhesive failure [34]. The results of the adhesion test for samples are shown in Fig. 10(S1–S5). Compared to the VD3195 standard in Fig. 2, the adhesion of all samples was acceptable as only a few cracks formed in the thin films of each sample. However, there were more cracks in the S4 sample, which spread around the indented traces. This indicates that sample S4 had a muscular film strength, but the lamination that occurred was quite large. The delamination formed was due to the low adhesion properties of the film. The adhesion of thin films is influenced by many factors, such as the roughness and cleanliness of the substrate, the films' structure, and the films' mechanical properties [35]. The results of this adhesion are in accordance with hardness test data, which show that S4 has the lowest hardness.
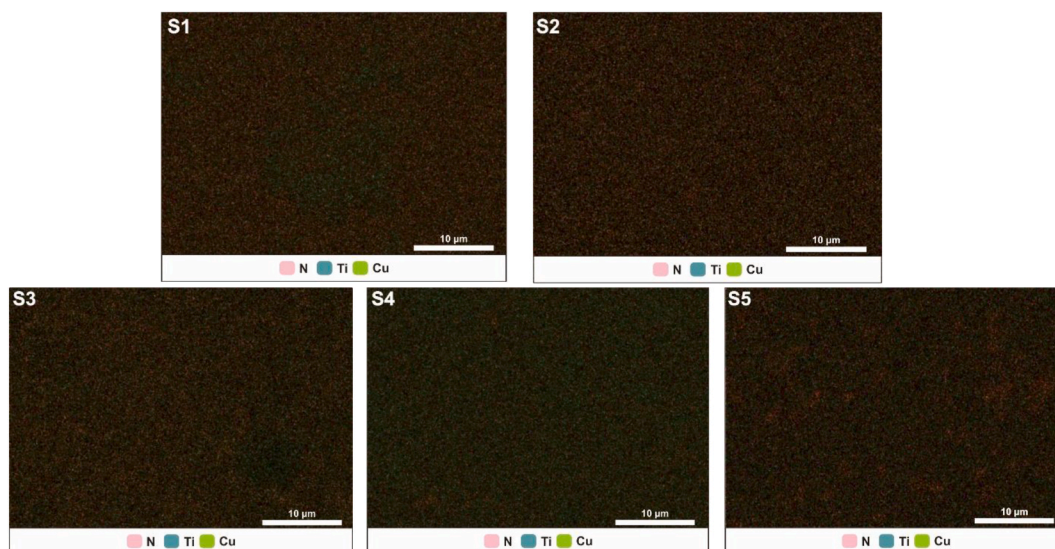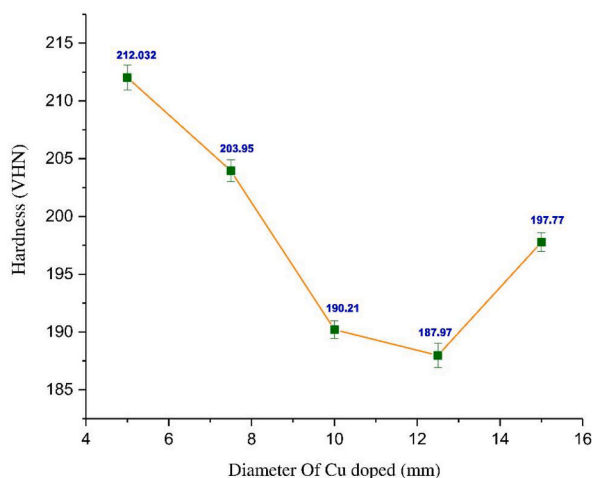
Fig. 8. EDS Mapping of sample S1–S5.

Fig. 9. Vickers hardness Ti–Cu–N films sample S1–S5.

3.3. Antibacterial properties

Fig. 11 describes the number of bacterial colonies in samples S1–S5. The samples were tested using *Staphylococcus aureus* bacteria with the spread plate method, then the number of colonies was calculated using the Colony Counter. Bacteria had contact with samples before inoculation for 1 h. *S. Aureus* bacteria was chosen because *Staphylococcus aureus* is the most dominant bacteria causing implant infections [36]. Based on photos of the colonies, bacteria that can survive appear in the form of white dots. Table 3 describes the number of bacterial colonies that grew and antibacterial effectiveness, presented as a percentage, of samples S1–S5. There was a significant reduction in the number of colonies from S1 to S5. The reduction in the number of colonies occurred due to the presence of Cu on the sample's surface. In S4–S5, no bacteria grew because all the bacteria had died [37], which was confirmed by SEM-EDS data. Based on Fig. 4, EDS Cu increases when the diameter of the doping is enlarged. Cu ions in the sample are released when bacteria come into contact with the sample's surface. The Cu damages bacteria by penetrating [3] negatively charged bacterial cell walls to enter the cell [37] and then interacting with the bacterial thiol protein and enzymes; thus, causing the bacteria to die [16,38]. Despite a highest dosage of copper within films would provide most augmented antibacterial properties, a balance between this property and other basic performance is critical for selection of the optimum concentration of copper into the films [39].
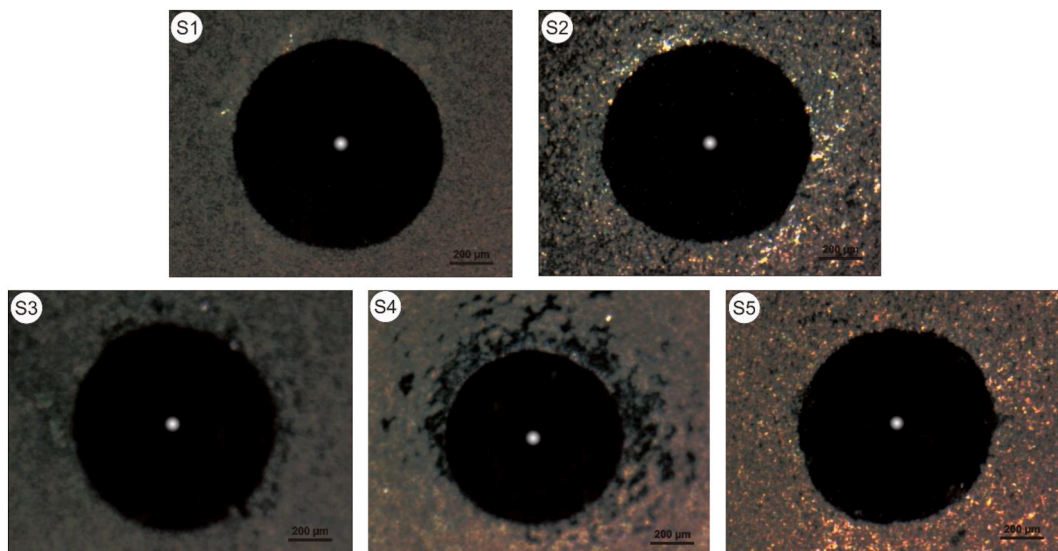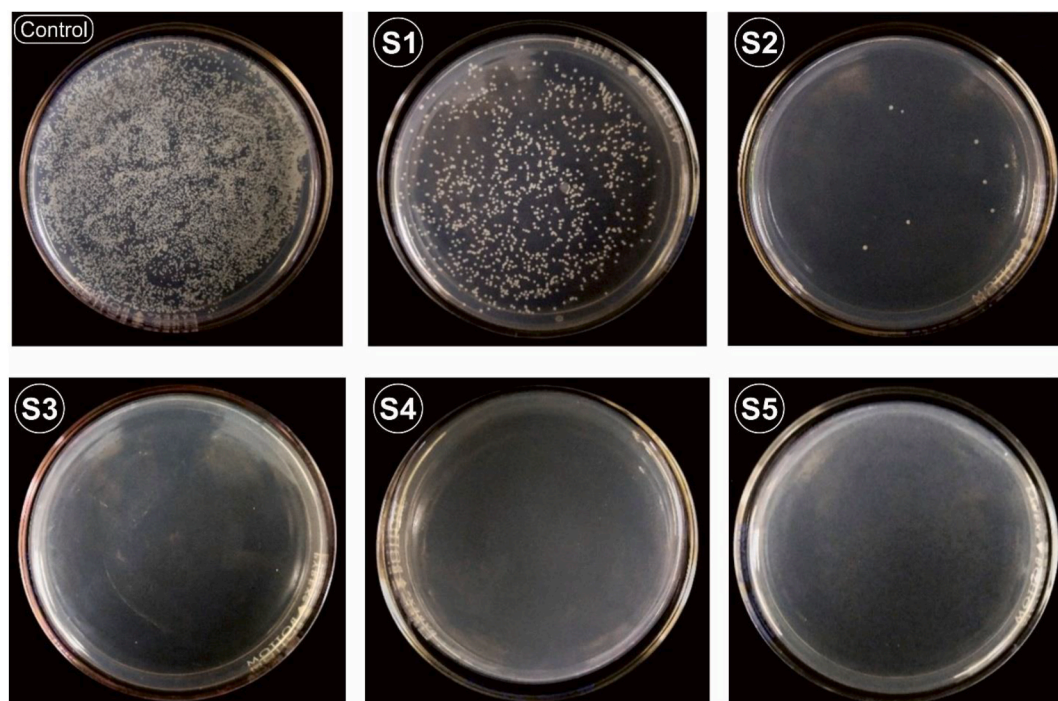
Fig. 10. Rockwell C imprints from sample S1–S5.

Fig. 11. Photos of colony forming units of viable *S. Aureus* after being in contact with control (SS316L without film) and S1–S5.

4. Conclusion

Ti–Cu–N films with various Cu contents were successfully grown using the reactive technique of DC sputtering. XRD demonstrated the formation of the crystalline phases FCC TiN and FCC Cu. Mechanical observations showed that the amount of Cu strongly influences the hardness of the Ti–Cu–N layer. The Vickers hardness number for S1–S4 decreased, but the values were still above the raw material hardness value. SS 316 L with Ti–Cu–N film has been observed to give an extraordinary increase in antibacterial activity. SEM-EDS confirmed that, in the presence of greater amounts of Cu, more S. Aureus bacteria dies.

Table 3
The bacterial test result for sample S1–S5.

Samples	Colony-Forming Unit (CFU) for *S.Aureus*	Reduction Of *S.Aureus* (%)
Raw	$1,102 \times 10^3$	0
S1	$4,6 \times 10^2$	58,2
S2	<10	99,3
S3	<10	99,8
S4	<10	99,9
S5	<10	99,9

Author contribution statement

Ihwanul Aziz, Yusril Yusuf: Conceived and designed the experiments; Performed the experiments; Analyzed and interpreted the data; Contributed reagents, materials, analysis tools or data; Wrote the paper.

Emy Mulyani: Analyzed and interpreted the data; Contributed reagents, materials, analysis tools or data; Wrote the paper.

Data availability statement

Data associated with this study has been deposited at https://storage2k.batan.go.id/index.php/s/c5k3FD6MFSTaLwg.

Additional information

No additional information is available for this paper.

Declaration of competing interest

We wish to confirm that there are no known conflicts of interest associated with this publication and there has been no significant financial support for this work that could have influenced its outcome.

We confirm that the manuscript has been read and approved by all named authors and that there are no other persons who satisfied the criteria for authorship but are not listed. We further confirm that the order of authors listed in the manuscript has been approved by all of us.

We confirm that we have given due consideration to the protection of intellectual property associated with this work and that there are no impediments to publication, including the timing of publication, with respect to intellectual property. In so doing we confirm that we have followed the regulations of our institutions concerning intellectual property.

We understand that the Corresponding Author is the sole contact for the Editorial process including Editorial Manager and direct communications with the office. He is responsible for communicating with the other authors about progress, submissions of revisions and final approval of proofs. We confirm that we have provided a current, correct email address which is accessible by the Corresponding Author.

References

[1] C. Morsiya, A Review on Parameters affecting Properties of Biomaterial SS 316L, 2020, pp. 2204–2253, https://doi.org/10.1080/14484846.2020.1752975.
[2] E. Zhang, X. Zhao, J. Hu, R. Wang, S. Fu, G. Qin, Antibacterial metals and alloys for potential biomedical implants, Bioact. Mater. 6 (2021) 2569–2612, https://doi.org/10.1016/j.bioactmat.2021.01.030.
[3] X. Zhang, X. Huang, Y. Ma, N. Lin, A. Fan, B. Tang, Bactericidal behavior of Cu-containing stainless steel surfaces, Appl. Surf. Sci. 258 (2012) 10058–10063, https://doi.org/10.1016/j.apsusc.2012.06.074.
[4] J. H. Hsieh, Antibacteria and Anti-wear TaN-(Ag,Cu) Nanocomposite Thin films Deposited on Polyether Ether Ketone.pdf, (2015).
[5] X.Y. Luo, D.L. Ma, P.P. Jing, Y.L. Gong, Y. Zhang, F.J. Jing, Y.X. Leng, In vitro analysis of cell compatibility of TiCuN films with different Cu contents, Surf. Coating. Technol. 408 (2021), https://doi.org/10.1016/j.surfcoat.2020.126790.
[6] J. Li, H. Zhang, A. Fan, B. Tang, Tribological properties characterization of Ti/Cu/N Thin films prepared by DC magnetron sputtering on titanium alloy, Surf. Coating. Technol. 294 (2016) 30–35, https://doi.org/10.1016/j.surfcoat.2016.03.043.
[7] P. Balashabadi, M.M. Larijani, E. Jafari-Khamse, H. Seyedi, The role of Cu content on the structural properties and hardness of TiN –Cu nanocomposite film, J. Alloys Compd. 728 (2017) 863–871, https://doi.org/10.1016/j.jallcom.2017.08.267.
[8] P.J. Kelly, H. Li, P.S. Benson, K.A. Whitehead, J. Verran, R.D. Arnell, I. Iordanova, Comparison of the tribological and antimicrobial properties of CrN/Ag, ZrN/Ag, TiN/Ag, and TiN/Cu nanocomposite coatings, Surf. Coating. Technol. 205 (2010) 1606–1610, https://doi.org/10.1016/j.surfcoat.2010.07.029.

[9] A. Dziedzic, W. Bochnowski, S. Adamiak, Szyller, J. Cebulski, I. Virt, M. Kus-Liśkiewicz, M. Marzec, P. Potera, A. Żaczek, B. Zdeb, Structure and antibacterial properties of Ag and N doped titanium dioxide coatings containing Ti2.85O4N phase, prepared by magnetron sputtering and annealing, Surf. Coating. Technol. 393 (2020), 125844, https://doi.org/10.1016/j.surfcoat.2020.125844.

[10] C.L. c J.H. Hsieh a, *, T.H. Yeh a, S.Y. Hung a, S.Y. Chang b, W. Wub, Antibacterial and Tribological Properties of TaN–Cu, TaN–Ag, and TaN–(Ag,Cu) Nanocomposite Thin Films, 2012, pp. 2999–3003, https://doi.org/10.1016/j.materresbull.2012.04.101.

[11] A. Ewald, C. Käppel, E. Vorndran, C. Moseke, M. Gelinsky, U. Gbureck, The effect of Cu(II)-loaded brushite scaffolds on growth and activity of osteoblastic cells, J. Biomed. Mater. Res., Part A 100 A (2012) 2392–2400, https://doi.org/10.1002/jbm.a.34184.

[12] P. Wang, Y. Yuan, K. Xu, H. Zhong, Y. Yang, S. Jin, K. Yang, X. Qi, Biological applications of copper-containing materials, Bioact. Mater. 6 (2021) 916–927, https://doi.org/10.1016/j.bioactmat.2020.09.017.

[13] A. Jacobs, G. Renaudin, C. Forestier, J.M. Nedelec, S. Descamps, Biological properties of copper-doped biomaterials for orthopedic applications: a review of antibacterial, angiogenic and osteogenic aspects, Acta Biomater. 117 (2020) 21–39, https://doi.org/10.1016/j.actbio.2020.09.044.

[14] D. Mitra, E.T. Kang, K.G. Neoh, Antimicrobial copper-based materials and coatings: potential multifaceted biomedical applications, ACS Appl. Mater. Interfaces 12 (2020) 21159–21182, https://doi.org/10.1021/acsami.9b17815.

[15] F. Heidenau, W. Mittelmeier, R. Detsch, M. Haenle, F. Stenzel, G. Ziegler, H. Gollwitzer, A novel antibacterial titania coating: metal ion toxicity and in vitro surface colonization, J. Mater. Sci. Mater. Med. 16 (2005) 883–888, https://doi.org/10.1007/s10856-005-4422-3.

[16] H. Wu, X. Zhang, X. He, M. Li, X. Huang, R. Hang, B. Tang, Wear and corrosion resistance of anti-bacterial Ti-Cu-N coatings on titanium implants, Appl. Surf. Sci. 317 (2014) 614–621, https://doi.org/10.1016/j.apsusc.2014.08.163.

[17] A. Rahmati, Reactive DC magnetron sputter deposited Ti-Cu-N nano-composite thin films at nitrogen ambient, Vacuum 85 (2011) 853–860, https://doi.org/10.1016/j.vacuum.2010.12.010.

[18] H. Wang, X. Shu, M. Guo, D. Huang, Z. Li, X. Li, B. Tang, Structural, tribological and antibacterial activities of Ti-Cu-N hard coatings prepared by plasma surface alloying technique, Surf. Coating. Technol. 235 (2013) 235–240, https://doi.org/10.1016/j.surfcoat.2013.07.038.

[19] X.Q. Wang, Y.H. Zhao, B.H. Yu, J.Q. Xiao, F.Q. Li, Deposition, structure and hardness of Ti-Cu-n hard films prepared by pulse biased arc ion plating, Vacuum 86 (2011) 415–421, https://doi.org/10.1016/j.vacuum.2011.08.015.

[20] C. Peng, Y. Zhao, S. Jin, J. Wang, R. Liu, H. Liu, W. Shi, S.K. Kolawole, L. Ren, B. Yu, K. Yang, Antibacterial TiCu/TiCuN multilayer films with good corrosion resistance deposited by axial magnetic field-enhanced arc ion plating, ACS Appl. Mater. Interfaces 11 (2019) 125–136, https://doi.org/10.1021/acsami.8b14038.

[21] J. Wang, B. Zhao, G. Li, K. Yang, J. Yu, X. Yang, D. Zhan, Study of TiCu/TiCuN multilayer films with antibacterial activity, Mater. Technol. 35 (2020) 475–482, https://doi.org/10.1080/10667857.2019.1699269.

[22] B.H. Priyambodo, V. Malau, P.T. Iswanto, T. Sujitno, Suprapto, The influence of TiN-sputtering on hardness and corrosion rate of AISI 304 for biomaterials application, J. Corrosion Sci. Eng. 20 (2017) 1–8.

[23] N. Vidakis, A. Antoniadis, N. Bilalis, The VDI 3198 Indentation Test Evaluation of a Reliable Qualitative Control for Layered Compounds, vol. 144, 2003, pp. 481–485, https://doi.org/10.1016/S0924-0136(03)00300-5.

[24] Y. Fan, D. Xie, D. Ma, F. Jing, D.T.A. Matthews, R. Ganesan, Y. Leng, Evaluation of the crystal structure and mechanical properties of Cu doped TiN films, Coatings 12 (2022) 652, https://doi.org/10.3390/coatings12050652.

[25] A. Rahmati, K. Ahmadi, Effect of sputtering power on structural, morphological, chemical, optical and electrical properties of Ti:Cu3N nano-crystalline thin films, EPJ Appl. Phys. 60 (2012), https://doi.org/10.1051/epjap/2012120247.

[26] V.S. Smentkowski, Trends in sputtering, Prog. Surf. Sci. 64 (2000) 1–58, https://doi.org/10.1016/S0079-6816(99)00021-0.

[27] H.P. Ng, P. Nandwana, A. Devaraj, M. Samblanet, S. Nag, P.N.H. Nakashima, S. Meher, C.J. Bettles, M.A. Gibson, H.L. Fraser, B.C. Muddle, R. Banerjee, Conjugated precipitation of twin-related α and Ti2Cu phases in a Ti-25V-3Cu alloy, Acta Mater. 84 (2015) 457–471, https://doi.org/10.1016/j.actamat.2014.10.053.

[28] C. Xin, N. Wang, Y. Chen, B. He, Q. Zhao, L. Chen, Y. Tang, B. Luo, Y. Zhao, X. Yang, Biological corrosion behaviour and antibacterial properties of Ti-Cu alloy with different Ti2Cu morphologies for dental applications, Mater. Des. 215 (2022), 110540, https://doi.org/10.1016/j.matdes.2022.110540.

[29] N. Malachowa, F.R. Deleo, Mobile genetic elements of Staphylococcus aureus, Cell. Mol. Life Sci. 67 (2010) 3057–3071, https://doi.org/10.1007/s00018-010-0389-4.

[30] V. Jokanović, N. Bundaleski, B. Petrović, M. Ferarra, B. Jokanović, S. Živković, I. Nasov, Detailed phisyco-chemical characterization of the multilayered thin films based on titanium oxynitride and copper doped titanium nitride obtained by different PVD techniques, Vacuum 195 (2022), https://doi.org/10.1016/j.vacuum.2021.110708.

[31] L. Wang, D.O. Northwood, X. Nie, J. Housden, E. Spain, A. Leyland, A. Matthews, Corrosion properties and contact resistance of TiN, TiAlN and CrN coatings in simulated proton exchange membrane fuel cell environments, J. Power Sources 195 (2010) 3814–3821, https://doi.org/10.1016/j.jpowsour.2009.12.127.

[32] Z. Tan, Y. Shi, B. Xing, Y. Hou, J. Cui, S. Jia, The antimicrobial effects and mechanism of ε-poly-lysine against Staphylococcus aureus, Bioresour. Bioprocess. 6 (2019), https://doi.org/10.1186/s40643-019-0246-8.

[33] A. Nemati, M. Saghafi, S. Khamseh, E. Alibakhshi, P. Zarrintaj, M.R. Saeb, Magnetron-sputtered TixNy thin films applied on titanium-based alloys for biomedical applications: composition-microstructure-property relationships, Surf. Coating. Technol. 349 (2018) 251–259, https://doi.org/10.1016/j.surfcoat.2018.05.068.

[34] W. Heinke, A. Leyland, A. Matthews, G. Berg, C. Friedrich, E. Broszeit, Evaluation of PVD nitride coatings, using impact, scratch and Rockwell-C adhesion tests, Thin Solid Films 270 (1995) 431–438, https://doi.org/10.1016/0040-6090(95)06934-8.

[35] J.M. Lackner, W. Waldhauser, M. Schwarz, F. Collins, D. Burtner, Adhesion Improvement of PVd Coatings by Plasma Treatment with Linear Anode Layer Ion Sources, 2007. Vacuum.

[36] M.A. Mini-review, B. Wildemann, K.D. Jandt, Infections @ trauma/orthopedic implants : recent advances on, Materials 14 (2021) 1–11, https://doi.org/10.3390/ma14195834.

[37] J. Chen, Z. He, J. Liu, Y. Wang, M. Hodgson, W. Gao, Antibacterial anodic aluminium oxide-copper coatings on aluminium alloys: preparation and long-term antibacterial performance, Chem. Eng. J. 461 (2023) 141873, https://doi.org/10.1016/j.cej.2023.141873.

[38] J. Liu, F. Li, C. Liu, H. Wang, B. Ren, K. Yang, E. Zhang, Effect of Cu content on the antibacterial activity of titanium-copper sintered alloys, Mater. Sci. Eng. C 35 (2014) 392–400, https://doi.org/10.1016/j.msec.2013.11.028.

[39] P.B. Milan, S. Khamseh, P. Zarrintaj, B. Ramezanzadeh, M. Badawi, S. Morisset, H. Vahabi, M.R. Saeb, M. Mozafari, Copper-enriched diamond-like carbon coatings promote regeneration at the bone–implant interface, Heliyon 6 (2020), e03798, https://doi.org/10.1016/j.heliyon.2020.e03798.